

In Search for Signs of Chaos in Branching Processes

Zhen Cao and Rudolph C. Hwa

Institute of Theoretical Science and Department of Physics, University of Oregon, Eugene, Oregon 97403-5203
(Received 3 April 1995)

For systems that involve particle production through branching processes, the concept of chaos is explored. The measures that can describe their behaviors are investigated. Monte Carlo simulation is used to generate events according to perturbative QCD and an Abelian model. It is shown how the measures proposed distinguish the two cases in ways that characterize the chaotic behavior.

PACS numbers: 13.85.Hd, 05.45.+b, 12.38.Bx, 24.60.Lz

It has been known for some time that the nonlinear, non-Abelian dynamics of the classical Yang-Mills field has chaotic solutions [1,2]. More recently, it has been shown by lattice calculation that the classical non-Abelian gauge theory generally exhibits deterministic chaos and that the Lyapunov exponents can be numerically determined [3–5]. How to extend the investigation to the quantum theory is, however, unclear inasmuch as the notion of quantum chaos for dynamics is not well defined [6,7]. In this paper we take the first step in that direction, not just going into the quantum dynamics of a nonlinear theory, but into the realm of particle production of quantized fields.

In this uncharted territory we have very little guidance on what to study in our search for signs of chaos. It is not clear what a trajectory is in QCD, even less, the distance between two trajectories. What exactly is Kolmogorov entropy (well defined in classical dynamics [8]) is also unclear in the multiparticle production problem. Our first objective is therefore to find some measure that can play the role of distance between trajectories and some other quantity that conveys the loss of information in the final state.

In order to know whether or not we have found the right measures, it is necessary to test our ideas on different dynamical problems and show that the measures can effectively distinguish different characteristics. We shall therefore concentrate on two branching processes in particle production. One is the pure gluon theory in perturbative QCD; the other is a cascade model (to be referred to as the χ model) that has none of the features of the gauge theory. We shall regard the gluons (partons) as particles and ignore hadronization so that we may focus on the issue of chaoticity in the branching dynamics.

In either case we start with a parton having timelike virtuality Q^2 and use computer simulation to study the evolution of the system through branching. The Monte Carlo code generates the parton momentum distribution that, in the case of QCD, satisfy the Altarelli-Parisi evolution equations [9–11]. The splitting functions for the two cases are drastically different, and the ways the virtualities degrade are also different. They give rise to the diverse behaviors that emerge. The question is how

to find a quantitative measure of the diversity that is useful from the point of view of chaoticity.

One of the difficulties in the problem posed is that time is not an explicit variable when calculating momentum distribution. Moreover, with the number of degrees of freedom increasing in the cascade process, there is no obvious way to generalize the definition of a trajectory in classical dynamics. However, branching has an irrefutable physical notion of the direction of time, and parton multiplicity n increases with time as long as we consider only tree diagrams (without recombination), which we do. Thus we take two conjugate views: the “temporal” development (parametrized by n), without regard to the parton momenta, and the “geometrical” characteristics in the momentum space at the end of the evolution. In some rough sense this corresponds to the two views of the classical systems that are related by ergodicity.

Concerning trajectory and distance between trajectories, our thinking is as follows. The classical field intensity is replaced in the quantum case by the number n of quanta, and the distance between two field configurations can be represented by the variance, D^2 , of the n distribution, P_n . This distribution arises after repeated simulation from the same initial condition, i.e., a fixed initial virtuality Q^2 . Quantum fluctuation is enough to replace the small variation of the initial condition in classical dynamics. With the average $\langle n \rangle$ regarded as a measure of the evolution time, D^2 as a function of $\langle n \rangle$ can then be regarded as the quantum analog of the classical distance function $d(t)$. This $\langle n \rangle$ is the average multiplicity, not just in the final state, but along the evolution process.

More precisely, let us focus on one event and use a tree to represent a particular branching process. Regardless of the virtuality q^2 of any line, all vertices of the same generation are put at the same branching level, and a label i is given to each generation between two levels, starting with $i = 0$ for the initial parton at Q^2 . By ignoring q^2 in the genealogy of the tree, we are emphasizing topology and overlooking momenta. Let n_i denote the number of partons at the i th generation. We shall use the event averaged $\langle n_i \rangle$ in lieu of time, although a simple linear or exponential relationship between the two is not expected.

In fact, $\langle n_i \rangle$ may not increase monotonically with i , even if n_i does; in such a case we use only the increasing portion. For the measure that plays the role of distance, we define the normalized variance

$$V_i = (\langle n_i^2 \rangle - \langle n_i \rangle^2) / \langle n_i \rangle^2. \quad (1)$$

This differs from the second cumulant moment K_2 by a term $-1/\langle n_i \rangle$, and it is better because K_2 can become negative (thus precluding log-log plots), while V_i is always positive. A rapid increase of V_i with $\langle n_i \rangle$ can be interpreted as the analog of the “divergence of nearby trajectories” in classical dynamics. Clearly, if V_i remains constant or decreases, one does not become more ignorant about the state of the system as it evolves, and thus it cannot be regarded as exhibiting chaotic behavior.

For Monte Carlo simulation we follow the procedure described by Odorico [10]. For both pure-gauge QCD and the χ model, we start with virtuality Q^2 and end at Q_0^2 . The splitting function for $g \rightarrow gg$ is

$$P(z) = 6 \left[\frac{1-z}{z} + \frac{z}{1-z} + z(1-z) \right], \quad (\text{for QCD}), \quad (2)$$

where z is the momentum fraction of the daughter parton in the frame, where the mother parton’s momentum is 1. In terms of the Sudakov form factor $S(Q^2, Q_0^2)$, one can calculate the probability of emitting a resolvable gluon occurring between Q^2 and Q_0^2 ; when it occurs in the simulation at q^2 , then z is chosen to be in the range $z_0 \leq z \leq 1 - z_0$, where $z_0 = Q_0^2/q^2$. The daughters evolve separately from the maximum virtualities, $q_1^2 = zq^2$ and $q_2^2 = (1-z)q^2$, according to the same procedure as applied to the mother. The running coupling constant is, as usual, $\alpha_s(q^2) = 4\pi/11 \log(q^2/\Lambda^2)$ where we have set $N_c = 3$, $N_f = 0$ and shall use $\Lambda = 250$ MeV. Branching ceases when q^2 reaches Q_0^2 or below.

In the χ model we use the splitting function

$$P(z) = 6z(1-z) \quad (\text{for the } \chi \text{ model}). \quad (3)$$

There is no infrared or collinear divergence and, therefore, no evolution. Nevertheless, we introduce Q^2 dependence by requiring that the daughter virtualities be zq^2 and $(1-z)q^2$, when the mother virtuality is q^2 , and z can be any value between 0 and 1. We require branching to occur successively until the virtualities of all lines reach Q_0^2 . We consider this model because it exemplifies the Abelian dynamics without infrared and collinear divergences. Yet, the multiplicity of particles produced depends on Q^2 so that the result of branching can be compared with the non-Abelian case, although for very different Q/Q_0 .

We have simulated these two branching processes by running 10^5 events each, using $Q_0 = 1$ GeV. The results on V_i vs $\langle n_i \rangle$ are shown in the log-log plot in Fig. 1 for various values of Q/Q_0 indicated. While it is hard to produce high multiplicity in QCD unless Q/Q_0 is extremely large, particles are copiously produced in the χ

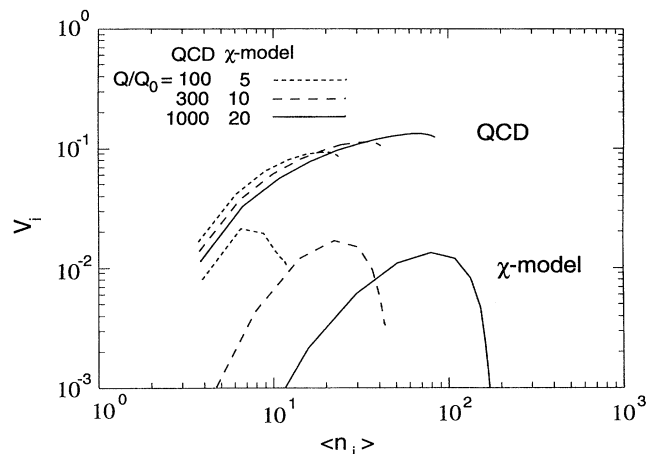


FIG. 1. Normalized variance vs average multiplicity at various generations in the branching processes.

model at moderate Q/Q_0 . The general features of V_i vs $\langle n_i \rangle$ for the two cases are markedly different. The QCD result shows a power-law increase in the high $\langle n_i \rangle$ range

$$V_i \propto \langle n_i \rangle^\kappa, \quad \kappa \approx 0.4, \quad (4)$$

where the exponent κ is approximately independent of Q^2 . The χ model, on the other hand, shows a rapid rise initially, but is followed by a precipitous drop after reaching a maximum. Indeed, the maximum V_i decreases with increasing Q^2 . Clearly, this is not a case that suggests chaotic behavior.

For gluon branching, the monotonic increase of V_i with $\langle n_i \rangle$ implies that, as the branching proceeds, the amount of particles produced in any event becomes more and more unpredictable. The power-law dependence may be regarded as the analog of the exponential increase with time of the distance between classical trajectories that are initially close by. However, there is no way to relate κ to the Lyapunov exponents, since among other differences the notion of time is not well defined here. By itself, $\kappa \approx 0.4$ does not indicate how chaotic the behavior is. There is a need for another measure of chaoticity.

If Fig. 1 is viewed as the analog of the description of the temporal behavior, another place to search for signs of chaos is in the phase space of the particles. As the system evolves, more and more information is lost on where the partons are (or more precisely, what their momenta are), therefore entropy increases, not only because of the increase of the number of particles, but also because of the dynamical fluctuations in their momenta. We therefore consider a multifractal description of that fluctuation and focus on the information dimension as a characterization of the entropy of the system [8].

Since at each vertex of branching a daughter’s momentum fraction z is known in the simulation, the momentum x of a final particle as a fraction of the initial particle is

therefore calculable by $x = \prod_i z_i$, where z_i is the momentum fraction of the descendant at the i th generation. Since the particle distribution $\rho(x)$ is highly peaked near $x = 0$, it is smoother to examine the distribution in the cumulative variable X , defined by [12]

$$X(x) = \int_{x_1}^x \rho(x') dx' / \int_{x_1}^{x_2} \rho(x') dx', \quad (5)$$

where x_1 and x_2 are two extreme points in the distribution $\rho(x)$, between which X varies from 0 to 1. In terms of X the inclusive distribution $\rho(X)$ is constant. For each event the fluctuation in X space is then studied by dividing the interval $0 \leq X \leq 1$ into M bins and calculating the factorial moments

$$f_q(M) = M^{-1} \sum_{j=1}^M n_j(n_j - 1) \cdots (n_j - q + 1), \quad (6)$$

where n_j is the multiplicity in the j th bin. After averaging over all events, the normalized factorial moment

$$F_q = \langle f_q \rangle / \langle f_1 \rangle^q \quad (7)$$

is known to contain no statistical fluctuations [13].

What interests us is its behavior near $q = 1$, where we can extract the information dimension D_1 . To that end, it is necessary to extend the definition of F_q in (6) to noninteger q . A method for achieving that without losing the attribute $F_q = 1$ for Poissonian fluctuation has recently been developed [14]. Using that method, we have calculated F_q for a continuous range of q , as shown in Fig. 2, for both QCD and the χ model. The results for the two cases are very different and provide a distinct contrast between them. They are in accord with the temporal behavior shown in Fig. 1 in that, for $q > 1$, $F_q < 1$ in the χ model, meaning that the distribution is sub-Poissonian, while $F_q > 1$ in QCD, indicating large fluctuations. The geometrical properties in the X space

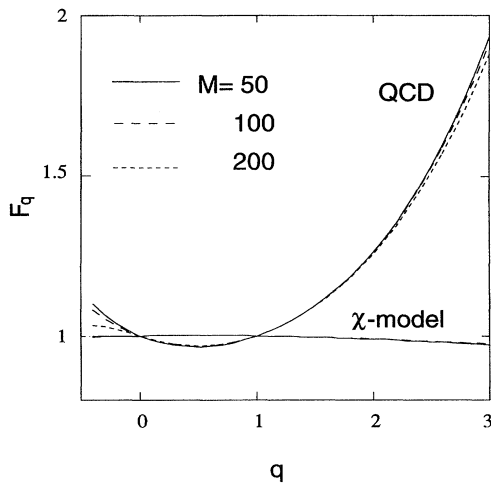


FIG. 2. Factorial moments of continuous order for various bin sizes. $Q/Q_0 = 10^3$ for QCD and $Q/Q_0 = 20$ for the χ model.

are not revealed until we investigate the M dependence. We find that in both cases F_q is not sensitive to M , as can be seen from the various lines in Fig. 2, corresponding to different M values. Thus the behavior has no interesting multifractal property: $D_1 \approx 1$ in both cases.

The origin of the lack of significant M dependence can be traced to F_q itself, where the event averaging cancels out the fluctuations. Event by event, the values of $F_q^e = f_q^e / (f_1^e)^q$ (where e labels an event) fluctuate greatly, especially when M is large. To quantify the degree of that fluctuation, we define event-averaged (vertical) moments of the (horizontal) F_q^e moments

$$C_{p,q}(M) = \langle F_q^p(M) \rangle / \langle F_q(M) \rangle^p, \quad (8)$$

where $\langle F_q^p \rangle = \mathcal{N}^{-1} \sum_e (F_q^e)^p$, \mathcal{N} being the total number of events. We then calculate $C_{p,q}(M)$ for $0 < p < 2$, and $q = 2, 3, 4$. It is found that $C_{p,q}(M)$ indeed exhibits significant M dependences, as shown in Fig. 3. In all cases of p and q , the χ model has smaller $C_{p,q}$ compared to QCD, implying smaller fluctuations of F_q^e . The M dependences do not show linearity over any extended range in the log-log plots, the best being from $M = 50-20$. In that range, we write

$$C_{p,q}(M) \propto M^{\psi_q(p)}. \quad (9)$$

From the slope $\psi_q(p)$ in the neighborhood of $p = 1$, we can calculate the index μ_q , defined by

$$\mu_q = \frac{d}{dp} \psi_q(p) |_{p=1}. \quad (10)$$

The result of our simulation yields for $q = 2, 3, 4$ the values $\mu_q = 0.0061, 0.054, 0.23$ in the case of QCD, and $0.0014, 0.010, 0.046$ in the χ model, respectively. Clearly, for each q , $\mu_q^{(QCD)}$ is significantly larger than $\mu_q^{(\chi)}$. We now give a physical interpretation of μ_q as an entropy index to be used as a new measure of the event fluctuation in branching processes.

If we define $P_q^e = F_q^e / \sum_e F_q^e$, and then define $H_{p,q} = \sum_e (P_q^e)^p$, we have an entropy in the event space

$$S_q = - \sum_e P_q^e \ln P_q^e = - \frac{d}{dp} \ln H_p |_{p=1}. \quad (11)$$

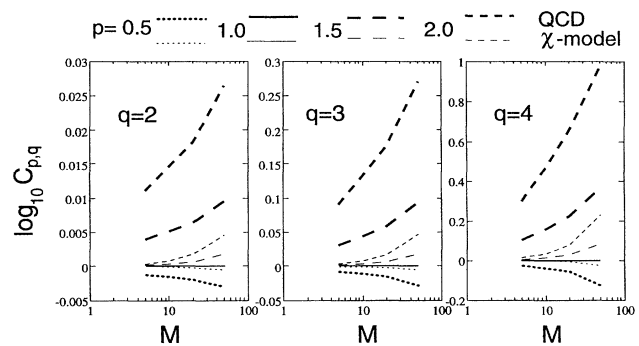


FIG. 3. $C_{p,q}$ vs M for various values of p and q . $Q/Q_0 = 10^3$ for QCD and $Q/Q_0 = 20$ for the χ model.

$H_{p,q}$ and $C_{p,q}$ can be related by their definitions, yielding

$$\frac{d}{dp} \ln C_{p,q}|_{p=1} = \ln \mathcal{N} - S_q. \quad (12)$$

From (9) and (10) we obtain

$$S_q = \ln(\mathcal{N} M^{-\mu_q}), \quad (13)$$

apart from a possible additive term, independent of \mathcal{N} and M . μ_q appears to be related to the information dimension; but it is not, because S_q is not the entropy defined in the X space, which is the one that is divided into M cells. The event space in which S_q is defined has not been partitioned into small cells. The meaning of (13) can be seen in two extreme cases: (a) If F_q^e is the same for every event, then $P_q^e = 1/\mathcal{N}$, and $S_q = \ln \mathcal{N}$; (b) if only one event has $F_q^e \neq 0$, and $F_q^e = 0$ in all others, then $S_q = 0$. Thus case (b) is more ordered in the event space than (a); that is, it is more disordered to spread out an observable (F_q^e in this case) over all events (even if $F_q^e = \text{const}$) than to confine it to a few events having nonzero values (analogous to the increase of entropy of an expanding gas). (The case of all $F_q^e = 0$ is excluded from consideration in order to render \hat{P}_q^e meaningful.) Thus S_q decreases when there are more events with $F_q^e = 0$, signifying more order in the event space. From (13), we see that μ_q is a measure of that decrease, which in turn implies more fluctuation in F_q^e .

At large M , only large spikes in small bins contribute to F_q^e , especially when q is large. Events with large spikes are rare. Consequently, the fluctuation in F_q^e from event to event becomes more pronounced with increasing q . That behavior is now quantified by μ_q . We may therefore use μ_q to characterize the spatial properties of the chaotic behavior of a branching process. We have, however, at this stage no quantitative criterion on how small μ_q must be in order to signify *no* chaotic behavior.

We can relate the classical and quantum problems in our description in the event space as follows. Consider a neighborhood N_ϵ around an initial point in phase space for a classical trajectory. For chaotic dynamics, starting the system from any point in N_ϵ leads to, after a sufficient length of time, widely different trajectories. We may regard \mathcal{N} of these trajectories in N_ϵ as corresponding to \mathcal{N} branching events, all with the same initial virtuality, but having different outcomes. $F_q^e(M)$ describes the final state of the system for the e th event, and μ_q describes the degree of fluctuation of F_q^e from event to event. Sufficiently large values for the index μ_q therefore signify chaotic behavior of the branching process.

In conclusion, we have found features pertaining to QCD branching that are not shared by the χ model, which represents Abelian branching. Because of the nonclassical nature of the system, we have had to search for new measures and observables. The dependence of V_i on $\langle n_i \rangle$ reveals the temporal behavior, while F_q , $C_{p,q}$, and μ_q describe the "spatial" properties. All these measures taken together give a collective description of the degree of chaoticity in a branching process. We have found that V_i increases with $\langle n_i \rangle$ in QCD, while it decreases for the χ model. The dependence of F_q on q are totally different for the two cases. $C_{p,q}$ and μ_q are much larger for QCD than for the χ model. These results suggest collectively that QCD branching is chaotic, while the χ model is not. Among the measures considered, V_i (and higher moments of n_i , which could also have been considered) vs $\langle n_i \rangle$ contains detailed information about the branching process from generation to generation, but it is not accessible to experiment. The others describe the characteristics of the final state and can be determined experimentally in most high-energy collisions. The entropy index μ_q is most unusual and deserves further investigation.

One of us (R. C. H.) is grateful to K. Geiger, B. L. Hao, S. G. Matinyan, and B. Müller for helpful discussions. This work was supported in part by the U.S. Department of Energy under Grant No. DE-FG06-91ER40637.

-
- [1] S. G. Matinyan *et al.*, Sov. Phys. JETP **53**, 421 (1981).
 - [2] S. G. Matinyan, Sov. J. Part. Nucl. **16**, 226 (1985), and references quoted therein.
 - [3] B. Müller and A. Trayanov, Phys. Rev. Lett. **68**, 3387 (1992).
 - [4] T. S. Biró, C. Gong, B. Müller, and A. Trayanov, Int. J. Mod. Phys. **C5**, 113 (1994).
 - [5] C. Gong, Phys. Lett. B **298**, 257 (1993); Phys. Rev. D **49**, 2642 (1994).
 - [6] M. Tabor, *Chaos and Integrability of Nonlinear Dynamics* (Wiley, New York, 1989).
 - [7] *Quantum Chaos*, edited by H. A. Cerdeira *et al.* (World Scientific, Singapore, 1991).
 - [8] H. G. Schuster, *Deterministic Chaos* (Physik-Verlag, Weinheim, 1984).
 - [9] A. Altarelli and G. Parisi, Nucl. Phys. **B126**, 298 (1977).
 - [10] E. Odorico, Nucl. Phys. **B172**, 157 (1989).
 - [11] B. R. Webber, Annu. Rev. Nucl. Part. Sci. **36**, 253 (1986).
 - [12] A. Białas and M. Gardzicki, Phys. Lett. B **252**, 483 (1990).
 - [13] A. Białas and R. Peschanski, Nucl. Phys. **B273**, 703 (1986); **B308**, 867 (1988).
 - [14] R. C. Hwa, Phys. Rev. D **51**, 3323 (1995).